AIP | The Journal of Chemical Physics

Matrix Infrared Spectrum and Bonding in the Dibromomethyl Radical

T. Granville Carver and Lester Andrews

Citation: The Journal of Chemical Physics **50**, 4223 (1969); doi: 10.1063/1.1670887
View online: http://dx.doi.org/10.1063/1.1670887
View Table of Contents: http://scitation.aip.org/content/aip/journal/jcp/50/10?ver=pdfcov
Published by the AIP Publishing

THE JOURNAL OF CHEMICAL PHYSICS VOLUME 50, NUMBER 10 15 MAY 1969

Matrix Infrared Spectrum and Bonding in the Dibromomethyl Radical*

T. GRANVILLE CARVER† AND LESTER ANDREWS‡

Chemistry Department and Center for Advanced Studies, University of Virginia, Charlottesville, Virginia 22901

(Received 13 December 1968)

Simultaneous condensation of bromoform and lithium atoms at high dilution in argon on a CsI window at 15°K produces new infrared absorptions which are assigned to lithium bromide and the dibromomethyl radical. The identity of dibromomethyl is confirmed by comparison of spectra obtained from $HCBr_3$, $DCBr_3$, and $HCBr_2Cl$ precursors reacting with lithium and sodium. These new absorptions are assigned to the antisymmetric H–C–Br bending and C–Br stretching modes and the symmetric C–Br vibration. The antisymmetric vibrational assignments are supported by product-rule and normal-coordinate calculations which give the potential constants $F_{55}=3.10\pm0.10$ mdyn/Å, $F_{56}=0.32\pm0.01$ mdyn/rad, and $F_{66}=0.50\pm0.05$ mdyn·Å/rad², while the symmetric C–Br mode yields an approximate force constant $F_{22}=3.7\pm0.4$ mdyn/Å. The C–Br valence force constants for bromomethyl radicals exceed normal C–Br values, while electronic stabilization for these radicals is indicated by bond dissociation energies. Similar results for chloromethyl radicals, in contrast to fluoromethyl radicals, suggest that $(p\text{–}d)\pi$ bonding between the free-radical carbon orbital and the *d* orbitals on chlorine and bromine might account for the stabilization of chloromethyl and bromomethyl radicals, which cannot occur for fluoromethyl radicals or molecules with completely satisfied valence.

INTRODUCTION

The dibromomethyl radical has been proposed as an intermediate in the peroxide-initiated reaction of bromoform with olefins[1] and in the pyrolysis of bromoform.[2] Although this radical has received relatively little attention in detailed mechanistic studies, its infrared spectrum and potential constants are of interest for comparison with those of the tribromomethyl[3] and dichloromethyl[4] radicals and with the potential constants of stable molecules.

EXPERIMENTAL

The 15°K refrigeration system, vacuum vessel, alakli-metal source, and experimental technique have been described earlier.[5,6] Isotopically enriched samples of lithium metal, 99.99% ^{7}Li and 95.6% ^{6}Li, 4.4% ^{7}Li (ORNL), and sodium metal (J. T. Baker, lump) were used without purification. Bromoform (Matheson, Coleman and Bell, spectroquality); bromoform-*d* (E. Merch, 99%) and chlorodibromomethane (Columbia Organic Chemicals, reagent) were outgassed by repeated freezing and thawing under vacuum and were vacuum distilled over adsorption alumina retaining the middle fraction. Argon (Air Products, 99.995%) and krypton (Matheson, research grade) were used without purification.

Samples of bromoform (matrix/reactant $=M/R=$ 200/1, 400/1, or 1000/1 in argon were simultaneously deposited with atomic beams of lithium or sodium (matrix/alkali $=M/A=200/1$ or 400/1) on a CsI window maintained at 15°K. Deposition times ranged from 12 to 24 h. Infrared spectra were recorded during and after sample deposition on a Beckman IR-12 filter-grating spectrophotometer in the 200–4000-cm^{-1} region. In selected experiments the deposited sample was warmed to near 45°K by bucking the refrigerator with electrical heaters on the low-temperature refrigeration stage after which it was recooled to 15°K. During this operation the window temperature was monitored with an Au–2.1% Co-vs-Cu thermocouple. Frequency accuracy is ±0.5 cm^{-1} with spectral slitwidths near 0.8 cm^{-1} at 1100, 900, and 700 cm^{-1} and 2.1 cm^{-1} at 500 cm^{-1}.

RESULTS

Bromoform

Infrared spectra in the 300–1300-cm^{-1} region for $HCBr_3$ (matrix/reactant $=M/R=200/1$) in solid argon at 15°K deposited without lithium, with ^{6}Li and with ^{7}Li (matrix/alkali $=M/A=200/1$) are presented in Fig. 1, and the observed frequencies and approximate relative intensities are listed in Table I. Comparison of the spectrum of $HCBr_3$ ($M/R=200/1$) deposited without alkali metal with the published spectrum[7] of $HCBr_3$ shows the presence of impurities (labeled I) with absorptions at 948, 752, 748, and 695 cm^{-1} in addition to the absorptions of $HCBr_3$, which are labeled P in the table and figures. When $HCBr_3$ is deposited with lithium, a number of new bands are observed, indicating that a reaction has occurred.

New bands at 504.0 cm^{-1} and at 438.5 and 431.0 cm^{-1} in the spectra of $HCBr_3$ in argon deposited with ^{7}Li agree well with the spectra of ^{7}LiBr monomer and

---

* Taken from the thesis submitted by T. Granville Carver to the Graduate School of the University of Virginia in partial fulfillment of the requirements of the degree of Doctor of Philosophy.

† Present address: Uniroyal Research, Wayne, N.J., 07470.

‡ To whom requests for reprints should be sent.

[1] M. S. Kharasch, E. V. Jensen, and W. H. Urry, J. Am. Chem. Soc. **69**, 1100 (1947).

[2] M. Szwarc and A. H. Sehon, J. Chem. Phys. **19**, 656 (1951).

[3] L. Andrews and T. G. Carver, J. Chem. Phys. **49**, 896 (1968).

[4] T. G. Carver and L. Andrews, J. Chem. Phys. **50**, 4235 (1969), following paper.

[5] L. Andrews, J. Chem. Phys. **48**, 972 (1968).

[6] T. G. Carver, Ph.D. thesis, University of Virginia, Charlottesville, Va., 1969.

[7] A. G. Meister, S. R. Rosser, and F. F. Cleveland, J. Chem. Phys. **18**, 346 (1950).

TABLE I. Absorption frequencies (cm^{-1}) of the products of the reaction of Li ($M/A=200/1$) with $HCBr_3$ ($M/R=200/1$) in an argon matrix.[a]

Figure 1 identification	$CHBr_3$ no Li	$CHBr_3$ ^{6}Li	$CHBr_3$ ^{7}Li
HA_1		1165.0 (1.32)	1165.0 (1.26)
P	1153.5 (100%T)	1153.5 (100%T)	1153.5 (100%T)
P	1147.0 (sh)	1147.0 (sh)	1147.0 (sh)
I	948.0 (0.10)	948.0 (0.12)	
HA_2		786.0 (3.00)	786.0 (2.66)
HA_2		778.5 (2.20)	778.5 (1.90)
U		772.5 (sh)	772.5 (sh)
P	767.5 (0.29)	767.0 (sh)	
HA'_2		765.0 (2.00)	765.0 (1.65)
HA'_2		760.5 (sh)	760.5 (sh)
I	752.0 (0.32)	752.5 (0.86)	752.5 (0.49)
I	748.5 (0.10)	748.5 (sh)	748.5 (sh)
C_2H_2		737.0 (0.28)	737.0 (0.14)
I	695.0 (3.08)	695.0 (2.62)	695.0 (2.04)
P	667.0 (100%T)	667.0 (100%T)	667.0 (100%T)
P	644.5 (0.99)	644.5 (0.66)	645.0 (0.39)
HA_3		633.0 (0.23)	633.0 (0.15)
U		619.0 (0.36)	620.0 (0.08)
P	543.5 (0.34)	542.0 (0%T)[b]	543.0 (0.34)
LC		521.0 (0.25)	486.5 (sh)
LiBr		504.0 (0.07)[c]	504.0 (2.86)
U		495.5 (0.18)	
$(LiBr)_2$		472.5 (0.80)	438.5 (0.76)
$(LiBr)_2$		463.0 (0.66)	431.0 (sh)
U			459.0 (0.55)
U		440.0 (0.11)	
U		421.0 (0.18)	
U		402.0 (0.16)	401.0 (0.47)

[a] Intensities (OD × cm^{-1}) are shown parenthetically.

[b] Parent plus ^{6}LiBr.

[c] Probably ^{7}LiBr due to the 4% ^{7}Li isotope present in the ^{6}Li.

dimer, respectively, in an argon matrix at 20°K recorded by Schlick and Schnepp.[8] Although the absorption of ^{6}LiBr is approximately coincident with ν_2 of $HCBr_3$ at 543.5 cm^{-1}, the formation of ^{6}LiBr when ^{6}Li is deposited with $HCBr_3$ is indicated by a large increase in the intensity of this band and a shift of the band peak to 542.0 cm^{-1} along with the appearance of new bands at 472.5 and 463.0 cm^{-1} which correspond to ^{6}LiBr dimer. Table II compares the observed lithium halide frequencies from the above and other experiments with those obtained by Schlick and Schnepp.[8]

Among the new features which appear in the spectra when $HCBr_3$ is codeposited with ^{6}Li or ^{7}Li are the pair of strong bands at 786.0 and 778.5 cm^{-1} which are labeled HA_2. At slightly lower frequencies a broad band with peaks at 765.0 and 760.5 cm^{-1} is designated by HA_2'. A new band at 1166.0 cm^{-1}, just above the hydrogen bending mode of the parent, is labeled HA_1 and a weak band at 633.0 cm^{-1} is labeled HA_3. Figure 2 shows the region of HA_1, HA_2, and HA_2' recorded under

---

[8] S. Schlick and O. Schnepp, J. Chem. Phys. 41, 463 (1964).

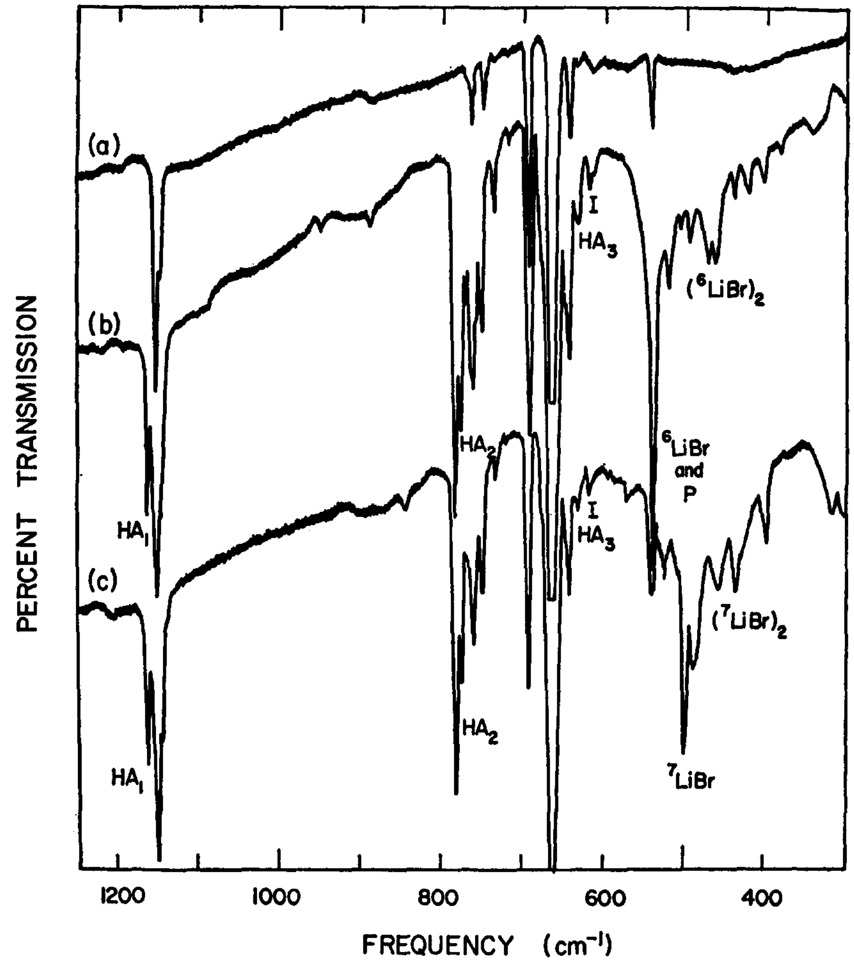

FIG. 1. Infrared spectra in the 300–1250-cm^{-1} spectral region for $HCBr_3$ ($M/R=200/1$) deposited in argon (a) without alkali metal, (b) with ^{6}Li ($M/A=200/1$), and (c) with ^{7}Li ($M/A=200/1$).

high-resolution conditions after deposition of $HCBr_3$ (200/1) with ^{6}Li (200/1).

The band at 737.0 cm^{-1} which appeared on initial warming of the heater and Knudsen cell, did not increase in intensity during sample deposition and is believed to be due to acetylene[9] probably produced by the reaction of lithium with traces of organic material inside the Knudsen cell. Additional weak absorptions are seen in some but *not all* experiments. These bands, which are usually weak and appear as shoulders or show a lithium isotope shift, are most often seen when high concentrations of precursor and alkali metal are used. Although the origin of these bands is unknown, they are thought to be due to aggregates or lithium-containing compounds which are not of interest here. Since little information about them is available from the spectra, these bands remain unidentified and are labeled U in Table I.

TABLE II. Infrared spectrum of LiBr in argon and krypton matrices (in cm^{-1}).

	^{6}LiBr		^{7}LiBr	
	This work	Schlick and Schnepp	This work	Schlick and Schnepp
	Argon matrix			
Monomer	···	561	···	521
	541.0	540	504.0	502
Dimer	472.5	470	···	449
	463.0	461	438.5	439
			431.0	430
	Krypton matrix			
Monomer	···	550	···	521
	530.5	528	494.5	492

Concentration Variation

When the concentration ratio of Ar/$HCBr_3$ is increased to 1000/1 while Ar/Li remains near 200/1, bands labeled HA$_1$, HA$_2$, and HA$_2'$ are observed but are less intense than in the 200/1 runs. It is noted that the intensity ratio of HA$_1$ to that of the high-frequency component of HA$_2$ (786.0 cm^{-1}) remains

---

[9] D. E. Milligan and M. E. Jacox, J. Chem. Phys. **47**, 5146 (1967).

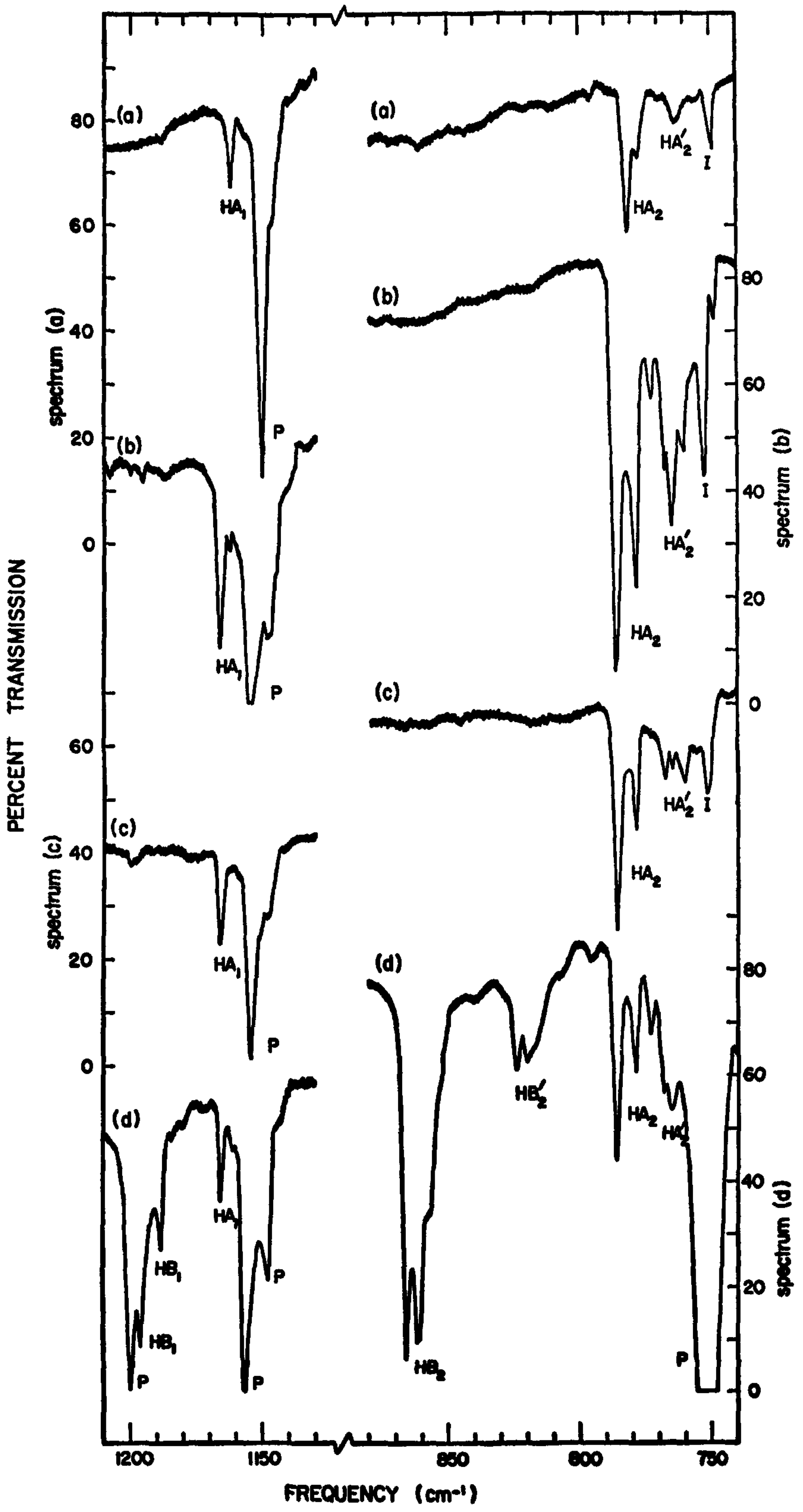

FIG. 2. Infrared spectra in the 740–880-cm^{-1} and 1130–1210-cm^{-1} spectral regions for (a) $HCBr_3$ ($M/R=200/1$) *in krypton* deposited with ^7Li ($M/A=200/1$), (b) $HCBr_3$ ($M/R=200/1$) deposited with ^6Li ($M/A=200/1$) in argon, (c) $HCBr_3$ ($M/R=400/1$) deposited with Na ($M/A=400/1$) in argon, and (d) $HCClBr_2$ ($M/R=200/1$) deposited with ^7Li ($M/A=200/1$) in argon.

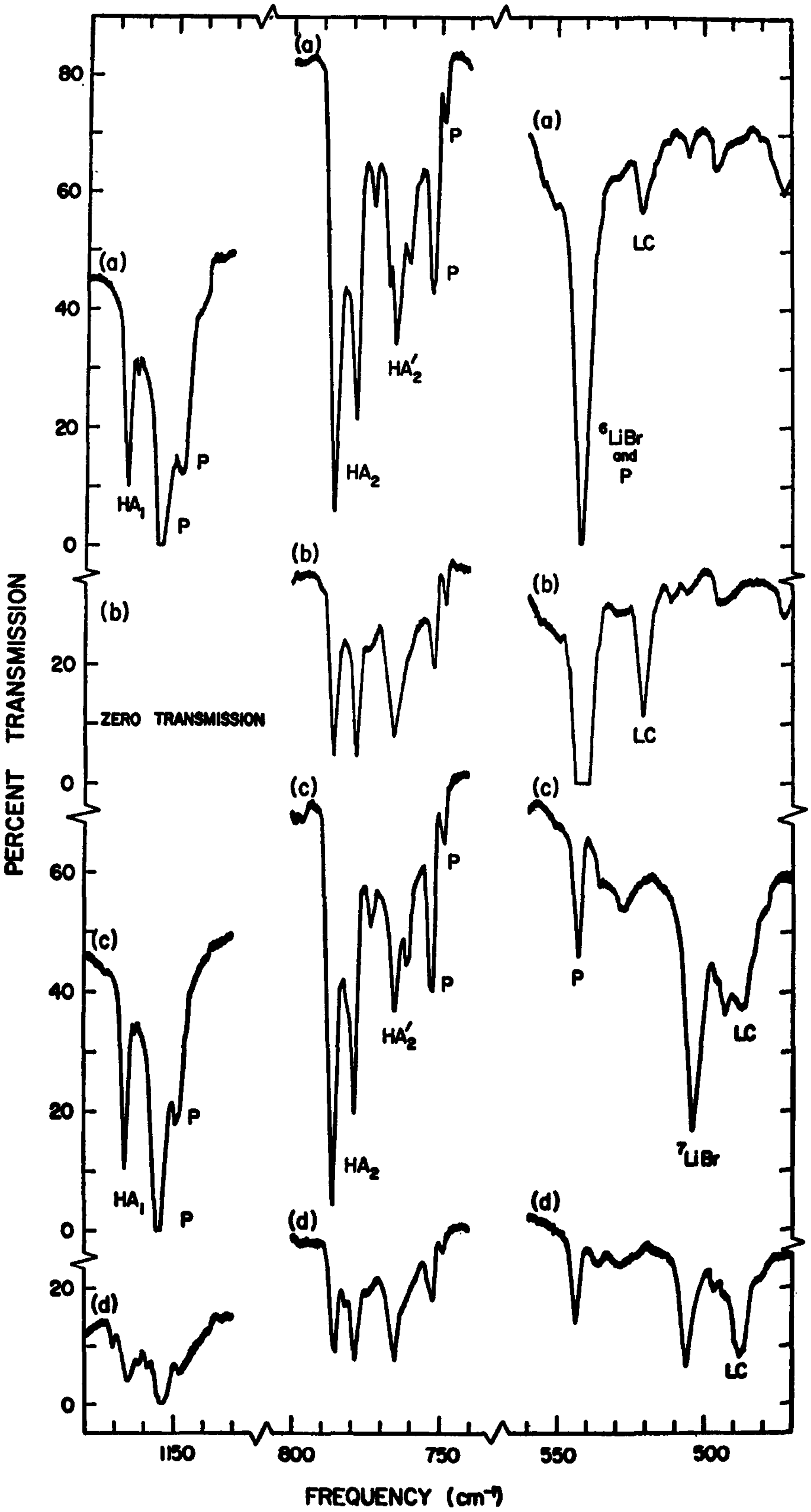

FIG. 3. Argon matrix spectra in the 470–560-cm⁻¹, 740–800-cm⁻¹, and 1130–1180-cm⁻¹ spectral regions for $HCBr_3$ ($M/R=200/1$) deposited with ^6Li ($M/A=200/1$), spectrum (a) before warming the sample and spectrum (b) after warming the sample to 35°K and recooling to 15°K; and for $HCBr_3$ ($M/R=200/1$) deposited with ^7Li ($M/A=200/1$), spectrum (c) before warming the sample and spectrum (d) after warming the sample to 35°K and recooling to 15°K.

TABLE III. Approximate intensity (OD×cm^{-1}) of the high-frequency component of HA_2 (786.0 cm^{-1}) and the ratio of the intensity of HA_1, low-frequency component of HA_2, and HA_3 to the intensity of the 786.0-cm^{-1} band observed in argon matrices.

Experiment			Intensity ratio		
Reactant (M/R)	Metal (M/A)	Intensity HA_2(h)[a]	HA_1/HA_2(h)	HA_2(l)[a]/HA_2(h)	HA_3/HA_2(h)
$CHBr_3$ (200/1)	^{6}Li (200/1)	3.00	0.44	0.73[b]	0.06
$CHBr_3$ (200/1)	^{7}Li (200/1)	2.66	0.47	0.71[b]	0.08
$CHBr_3$ (1000/1)	^{6}Li (200/1)	1.24	0.48	0.47	···
$CHBr_3$ (200/1)	Na (200/1)	1.06	0.44	0.49	···
$CHClBr_2$ (200/1)	^{6}Li (200/1)	0.81	0.44	0.49	···
$CHClBr_2$ (200/1)	^{7}Li (200/1)	0.68	0.46	0.50	···
$CHClBr_2$ (1000/1)	^{6}Li (200/1)	0.32	0.48	0.50	···

[a] HA_2(h) is the high-frequency component of HA_2 (786.0 cm^{-1}) and HA_2(l) is the low-frequency component (778.5 cm^{-1}).

[b] The measured intensity of HA_2(l) is too large because the band is overlapped by other strong absorptions.

approximately constant at 0.48 while the intensity ratio HA_2'/HA_2 decreased from 0.65 in the $M/R=200/1$ to 0.16 in the 1000/1 experiment. Table III lists the ratio of the intensities of the bands at 1166.0, 778.5, and 633.0 cm^{-1} to the intensity of the 786.0-cm^{-1} absorption in all experiments where these bands are observed.

Comparison of ^{6}Li, ^{7}Li, and Na

When lithium is replaced by sodium, bands HA_1 and HA_2 again appear with reduced intensity as is seen in Fig. 2. These bands show no measurable frequency shift with ^{6}Li, ^{7}Li, or Na. The bands labeled HA_2' also are present but are weak and broad.

Mixed Halogen Precursors

Experiments with $HCClBr_2$ as the precursor were performed at the same concentrations of parent and alkali metal as those used above for $HCBr_3$. These results show that both LiCl and LiBr are formed and that the bands labeled HA_1 and HA_2 are also present when $HCClBr_2$ is reacted with lithium while the band labeled HA_2' is likely obscured by the parent absorption. In addition, new bands at 1196.0 and 1188.0 cm^{-1} which are labeled HB_1, at 866.0, 861.0, and 857.0 cm^{-1} labeled HB_2, and at 823.5 and 820 cm^{-1} labeled HB_2' are seen in these spectra. These new absorptions were not observed with $HCBr_3$. Figure 2 shows spectra in the region from 770 to 880 cm^{-1} and from 1130 to 1210 cm^{-1} obtained from $HCClBr_2$ ($M/R=200/1$) deposited with ^{7}Li ($M/A=200/1$). When similar experiments are performed with $HCBrCl_2$, the bands HB_1 and HB_2 are also observed in the spectra; again the bands show the same structure and frequencies.[4]

Diffusion Experiments

When samples deposited at 15°K are warmed to between 35° and 45°K and recooled to 15°K, there is a pronounced growth in the formerly weak bands labeled LC at 521.0 and 486.5 cm^{-1} with ^{6}Li and ^{7}Li, respectively. The concomitant growth in HA_2' and decrease in HA_2 are also noted, and it is found that the lower-frequency component of HA_2 is relatively more intense after warmup than the higher-frequency component although both have decreased in intensity. In Fig. 3 spectra are shown from 470–560 cm^{-1}, 740–800 cm^{-1}, and 1130–1180 cm^{-1} for $HCBr_3$ ($M/R=200/1$) with ^{6}Li and ^{7}Li ($M/A=200/1$) both before and after warming the sample to allow diffusion.

Upon warmup of the $HCClBr_2$ experiments, bands labeled HA_1 and HA_2 show the same behavior as was observed in the $HCBr_3$ runs, and the bands HB_1, HB_2, and HB_2' exhibited similar behavior. The intensity of the higher-frequency component of HB_1 decreases more than the lower-frequency one, and the upper component of HB_2 decreases more than the lower-frequency pair. In the experiment with $HCClBr_2$ ($M/R=200/1$) and ^{6}Li ($M/A=200/1$), a weak band at 523.0 cm^{-1}, a few wavenumbers below the LiBr absorption, shows a striking increase in intensity. Unfortunately no spectra were obtained in this region after diffusion in the ^{7}Li run, and the warmup behavior of a similar band at 487.0 cm^{-1} was not observed. No bands were observed after diffusion in the $HCClBr_2$ or $HCBr_3$ experiments which were not present before warmup.

Krypton Matrix

Lithium-6 and lithium-7 ($M/A=200/1$) were deposited with $HCBr_3$ ($M/R=200/1$) in krypton and HA_1, HA_2, and HA_2' were found at 1162.0, 781.0, and 763.0 cm^{-1}, respectively, for ^{6}Li and at 1162.0, 781.5, and 763.5 cm^{-1} for ^{7}Li. As can be seen in Fig. 2, the absorption designated HA_2, which appears as a pair of bands in an Ar matrix, has only one peak with an unresolved shoulder in the Kr matrix.

The frequencies of LiBr in Kr are also compared with the results of Schlick and Schnepp in Table II. Bands LC were observed at 508.0 cm^{-1} with ^{6}Li and at 474.0 cm^{-1} with ^{7}Li and were found to increase in intensity on diffusion as in the Ar matrix.

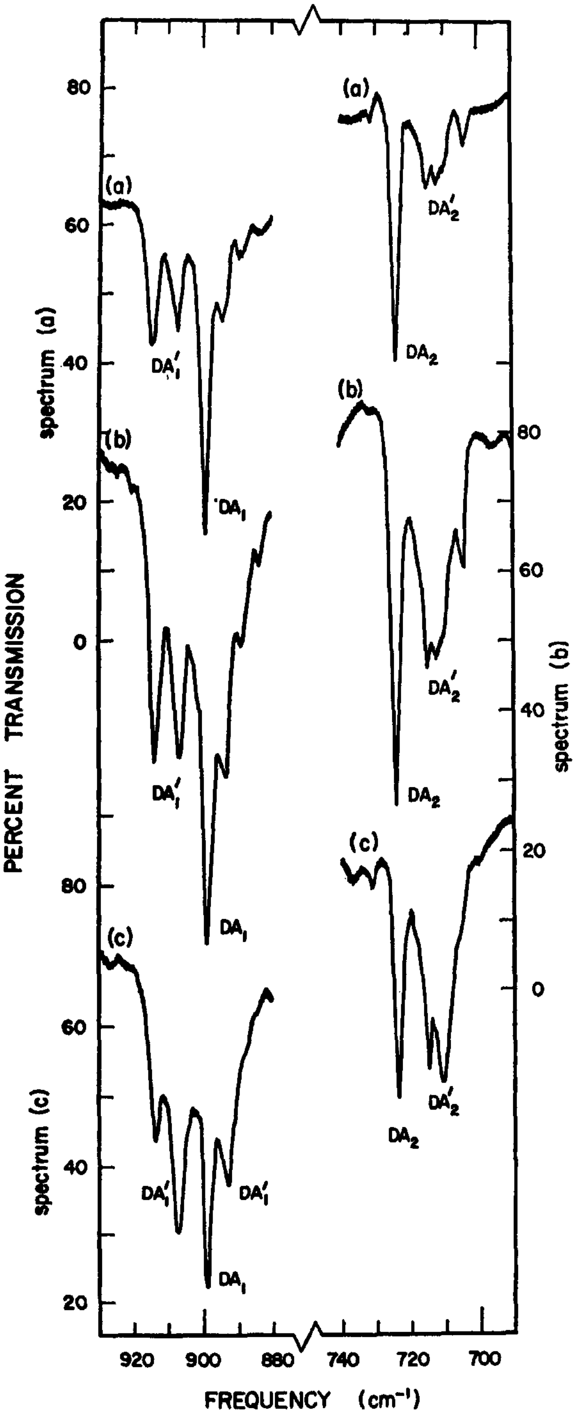

FIG. 4. Argon matrix spectra in the 690–740-cm^{-1} and 880–930-cm^{-1} spectral regions for (a) $DCBr_3$ ($M/R=1000/1$) deposited with ^{7}Li ($M/A=200/1$), (b) $DCBr_3$ ($M/R=200/1$) deposited with ^{6}Li ($M/A=200/1$), and (c) $DCBr_3$ ($M/R=200/1$) deposited with Na ($M/A=200/1$).

Bromoform-*d*

Experiments with $DCBr_3$ ($M/R=200/1$) with ^{6}Li, ^{7}Li, and Na ($M/A=200/1$) and without alkali metal were run in addition to $DCBr_3$ ($M/R=1000/1$) with ^{7}Li ($M/A=200/1$). Runs in which lithium was deposited with the $DCBr_3$ show the spectra of LiBr and a number of new absorptions which are also produced when Na is deposited with $DCBr_3$. The region around 900 cm^{-1} shows four new bands; the band at 898.5 cm^{-1} labeled DA_1 is the most optically dense band of this group in all experiments. The other three bands which are weakest in the ($M/R=1000/1$) experiment and much stronger in the Na runs are labeled DA_1' and do not show a constant intensity ratio with DA_1 as is seen in Fig. 4. There are also two new bands at 724.5 and 713 cm^{-1}. The 713-cm^{-1} band is broad and irregularly shaped in the experiments with Li and is resolved into a doublet at 714.5 and 710.0 cm^{-1} in Na runs. The band at 724.5 cm^{-1}, which does not shift in frequency with change in alkali metal is labeled DA_2, while the band at 713 cm^{-1}, which appears to maintain an approximately constant intensity ratio with bands designated by DA_1', is labeled DA_2'. A weak band at 616.5 cm^{-1} (DA_3) is also present in the spectra from ($M/R=200/1$) with both lithium isotopes and does not show an isotopic shift. Table IV shows the intensity of DA_2 (724.5 cm^{-1}) and the ratio of the intensities of the other bands to the intensity of DA_2. On warming the sample resulting from codeposition of $DCBr_3$ ($M/R=200/1$) and ^{6}Li ($M/Li=200/1$), a band labeled LC near 524 cm^{-1} grows strongly, and this is accompanied by a striking increase in intensity of DA_2' and a decrease in intensity of DA_2. Because of the coincidence of LC with the parent absorption at 525.0 cm^{-1} and the irregular shape of DA_2', quantitative measurement was not possible.

DISCUSSION

We wish to turn our attention to the identification, vibrational assignments, and normal-coordinate analysis of the molecular species responsible for the infrared absorptions described above.

Identification of HA and DA Species

The observation of LiBr in the spectrum recorded after codepositing lithium atoms and bromoform indicates that bromine abstraction by lithium does occur making $HCBr_2$ the likely product. In previous studies of reactions of alkali-metal atoms with CCl_4 and CBr_4, the primary reaction yielded the trihalomethyl radical[3,5] and the lithium halide. It seems reasonable to expect that the initial products of the reaction of bromoform with alkali-metal atoms would be the analogous free radical, $HCBr_2$, and the alkali halide.

It is first concluded that the species producing the absorptions HA and DA is highly reactive, since these bands decrease markedly in intensity on warming the

TABLE IV. Intensity (OD×cm^{-1}) of DA_2 (724.5 cm^{-1}) and the ratio of the intensities of other absorptions to the intensity of DA_2 observed in argon matrices.

Experiment		Intensity	Intensity ratio			
Reactant (M/R)	Metal (M/A)	DA_2	$DA_1'(h)^a/DA_2$	$DA_1'(m)^a/DA_2$	DA_1/DA_2	DA_3/DA_2
$DCBr_3$ (200/1)	^6Li (200/1)	1.30	1.08	1.12	2.10	0.23
$DCBr_3$ (200/1)	^7Li (200/1)	0.96	1.08	1.10	2.10	0.21
$DCBr_3$ (1000/1)	^7Li (200/1)	0.61	0.89	0.89	2.18	···
$DCBr_3$ (200/1)	Na (200/1)	0.62	1.33	2.60	2.19	···

[a] $DA_1'(h)$ is the high-frequency component of DA_1' (913.5 cm^{-1}), $DA_1'(m)$ is the middle-frequency component of DA_1' (906.0 cm^{-1}), and the low component of DA_1' is a shoulder at 893.0 cm^{-1}, the intensity of which could not be measured accurately.

matrix to 45°K. It is unlikely, although possible, that a stable molecule would exhibit this behavior.

As is seen from Tables III and IV, the ratio of the intensities of HA_1/HA_2, HA_3/HA_2 and DA_1/DA_2, DA_3/DA_2 is constant within experimental error; thus, these absorptions may be assigned to the same molecular species. Constant relative intensity is a necessary but not sufficient condition for the assignment of bands to the same species.

In all experiments in which they are observed, the bands HA_1, HA_2, HA_3 and DA_1, DA_2, DA_3 show no shift in frequency, within the experimental error of ±0.5 cm^{-1}, or variation in band shape with changes in the precursor, the concentration of the parent, or the alkali metal. If the species responsible for these absorptions contained an alkali-metal atom(s), a frequency shift would be expected when the alkali metal was varied from ^6Li to ^7Li to Na. Since no frequency shifts are found, the absorbing species likely does not contain an alkali-metal atom and probably is isolated from alkali-metal halides as well.

The production of the two intense bands, HA_1 and HA_2, seen in the $HCBr_3$ reactions, from the analogous reaction of $HCClBr_2$ with alkali metals indicates that the species responsible for these absorptions must be common to both of these precursors and that the mechanism of the reaction must be such that the species can be easily produced from both $HCBr_3$ and $HCClBr_2$. The presence of the bands HA_1 and HA_2 along with the spectrum of LiCl in spectra from the $HCClBr_2$-plus-Li experiments is strong chemical evidence that the species HA is the $HCBr_2$ radical and that it is produced in the primary step of the halocarbon–lithium reaction by simple abstraction of a halogen atom.

If the above hypothesis is valid, then the abstraction of a Br atom from $HCClBr_2$ should yield the free radical HCBrCl. Intense new bands labeled HB_1 and HB_2 are found, at frequencies higher than HA_1 and HA_2, respectively, in spectra resulting from reaction with $HCClBr_2$ (see Fig. 2). The HB absorber is not produced by the reaction of alkali metals with $HCBr_3$, but the HB absorptions are seen in spectra from the reaction with $HCBrCl_2$ (see following paper[4]) as well as $HCBr_2Cl$. Thus, the same arguments which were applied to $HCBr_2$ may be adopted for the HB absorber; it must be common to both $HCBr_2Cl$ and $HCBrCl_2$. It is concluded that the absorptions labeled HB_1 and HB_2 are due to HCBrCl.

It has been previously noted that in an argon matrix the spectral feature designated HA_1 is a pair of sharp bands separated by 7.5 cm^{-1} and that the 786.0-cm^{-1} component is more intense than the 778.5-cm^{-1} component before warmup while the reverse is found after diffusion. This frequency difference and the behavior on warmup are typical of site effects[10] often observed in matrix spectra; this pair of bands is likely due to a single vibrational mode of a species trapped in two nonequivalent sites in the argon matrix. With krypton as the matrix gas, only a single absorption is

TABLE V. New absorptions resulting from the reaction of lithium with bromoform and bromoform-*d* in an argon matrix.

Label	Frequency (cm^{-1})	Label	Frequency (cm^{-1})
Bromoform		Bromoform-*d*	
HA_1	1165.9	DA_1'	913.5
HA_2	786.0	DA_1'	906.0
HA_2	778.5	DA_1	898.4
HA_2'	765.0	DA_1'	893.0
HA_2'	760.5	DA_2	724.7
HA_3	633.0	DA_2'	713.0
		DA_3	616.5
Lithium-6		Lithium-7	
LC	521.0	LC	486.5

---

[10] G. C. Pimentel and S. W. Charles, Pure Appl. Chem. **7**, 111 (1963).

found at 781.0 cm^{-1} and this band is labeled HA_1 in Fig. 2. Thus, a dependence on the nature of the matrix is clearly demonstrated. Site effects have been found for CBr_3 radicals[3] and other reactive species such as $HCCl_2$.[4]

We conclude that the species causing the HA and DA absorptions are the $HCBr_2$ and $DCBr_2$ free radicals.

Identification of the HA′ and DA′ Species

Although compelling evidence has been presented linking the absorptions labeled HA and DA with the radicals $HCBr_2$ and $DCBr_2$, the origin of the bands HA′ and DA′, which lie in close proximity to the radical absorptions, has not been identified. The bands labeled DA_1' and DA_2' appear qualitatively to show corresponding changes under the various conditions of the experiments, and these bands are thought to be due to the same molecular species. No primed band is found in the vicinity of HA_1, but such a band might be obscured by the strong parent absorption just below HA_1. The primed absorptions do not maintain a constant intensity relative to the radical bands as the concentrations of Li and the precursor are varied, and they show independent behavior on warmup, sometimes increasing while the radical absorptions show a decrease. When Na is the alkali metal used, the primed absorptions show changes in intensity and band shape.

Several conclusions about the nature of the species responsible for the primed absorptions seem apparent. It appears that the species responsible for these bands is likely an aggregate or poorly isolated species since relatively less of this species is produced at low concentrations of precursor (high M/R). The similarity between the primed bands and the spectrum of the radical for both $HCBr_2$ and $DCBr_2$ suggests that the primed absorptions are due to a perturbed radical. The proximity of the primed bands to those of the radical further strengthens this argument, especially when it is noted that both HA_2 and HA_2' lie at somewhat higher than normal frequencies for C–Br vibrations.

The differences in the primed bands found upon comparison of results from Li and Na are evidence that the alkali metal or its halide may be the perturbing influence. We feel that the species producing the primed absorptions is a radical perturbed by or weakly bonded to an alkali halide since the alkali metal alone would be expected to bond to the radical producing much more drastic spectral changes (see, for example, Ref. 11). Further, the increase in the intensity of the primed bands on diffusion may be taken to infer that the absorptions are due to a weakly bonded complex.

In addition, bands in an Ar matrix at 521.0 cm^{-1} in the ^{6}Li runs and at 486.5 cm^{-1} in the ^{7}Li experiments which are labeled LC and show growth on warmup and similar bands in a Kr matrix may be due to LiBr complexed to the radical. Qualitatively, at least, these bands show approximately constant intensity ratios with the primed bands and similar growth on warmup. Force constant calculations, assuming that the LC bands are due to LiBr, yield excellent agreement between the observed and calculated lithium isotope shifts. No bands of LiBr in an argon or krypton matrix have been found at the frequencies of LC in our experience or in the work of Schlick and Schnepp.[8] Further, isolated LiBr is known to decrease in intensity on diffusion, in contrast to LC. We therefore surmise that the origin of the LC absorptions is likely the complexed LiBr which is weakly bonded to the radical. The force constants for the complexed LiBr (labeled LC) are smaller than for the unperturbed LiBr, and the agreement between the calculated and observed frequencies is not as good for LC as for LiBr. The lower frequency for the complexed LiBr may be due to a lower force constant corresponding to a weaker Li–Br bond or an increase in the effective reduced mass which would be expected in a complexed LiBr. The slightly poorer agreement between the frequencies suggests that the LiBr in the complex feels the effect of the mass of the radical.

Recently, Tan and Pimentel[12] have suggested the interaction between an alkali-metal halide and the methyl radical to explain certain features in spectra obtained from the reaction of CH_3Br and CH_3I with alkali metals. In this work, no absorptions were assigned to the complexed alkali halide vibrations. It seems likely that a higher concentration of radicals and LiBr was produced here than in the study by Tan and Pimentel, since $HCBr_3$ is expected to be more reactive toward alkali metals than the methyl halides. The higher concentration of radicals and LiBr should lead to a higher concentration of the complex which would allow the observation of the weak absorption assigned here to the complexed LiBr. It is interesting to note that a basic difference may exist between the radical–alkali halide complex suggested here and the methyl alkali halide proposed by Tan and Pimentel. Since $HCBr_2$ is expected to have a dipole moment in contrast to the methyl radical which is planar and has no dipole moment, dipole–dipole interaction is possible between the $HCBr_2$ radical and the alkali halide which has a large dipole moment. If dipole–dipole interaction is the origin of the perturbation, the alkali halide would lie parallel to the radical with its dipole moment opposed to that of the radical. Unfortunately, it is impossible to draw any conclusions about the structure of the complex from the observed spectra. It is, however, noteworthy that the frequency shifts

---

[11] L. Andrews and T. G. Carver, J. Phys. Chem. **72**, 1743 (1968).

[12] L. Y. Tan and G. C. Pimentel, J. Chem. Phys. **48**, 5202 (1968).

between the isolated and perturbed radicals are small and that little difference in perturbations was seen between LiBr and NaBr. No evidence of similar perturbations was found for CBr_3[3] or for CCl_3.[5]

Vibrational Assignments

Since the dibromomethyl radical has not been previously detected by physical methods, its structure is unknown. However, methyl itself is reported to be planar[13] while trifluoromethyl is pyramidal.[14] The electron spin resonance spectrum of difluoromethyl has been interpreted to suggest a pyramidal structure[14] with valence angles near 115°. The appearance of bands in the infrared spectra of trichloromethyl[5] and tribromomethyl[3] assigned to the symmetric carbon–halogen stretching vibration implies that these radicals are also nonplanar. By analogy, we suggest that the dibromomethyl radical is pyramidal with bond angles intermediate between tetrahedral and planar. Assuming that the C–Br bond distances and H–C–Br angles are identical, the radical has C_s symmetry. If the molecule is planar, it would belong to the C_{2v} point group. A nonlinear tetra-atomic molecule has six normal modes of vibration. For a pyramidal radical with C_s symmetry, four normal modes belong to the A' symmetry species and two to the A'' species, with all six modes infrared-allowed. The feature labeled HA_1 is at an appropriate frequency for assignment to the antisymmetric HCBr valence angle bending mode, ν_5 (A''), of the dibromomethyl radical while the absorption designated DA_1 is assigned to the same mode of dibromomethyl-*d*. The bands assigned to the antisymmetric C–Br stretching vibration, ν_6 (A''), have been designated HA_2 and DA_2 for $HCBr_2$ and $DCBr_2$, respectively.

The absorptions labeled HA_3 and DA_3 are assigned to the symmetric C–Br stretching motion, ν_2 (A′), of $HCBr_2$ and $DCBr_2$, respectively. Comparison of the spectrum of $HCBr_2$ with that of H_2CBr_2 in an Ar matrix (see Ref. 3) shows that HA_3 lies 50 cm^{-1} above the corresponding motion of H_2CBr_2 while HA_2 is about 136 cm^{-1} higher than the similar motion. Although product-rule calculations cannot be made, the 16.5-cm^{-1} deuterium shift of this band is reasonable, since the deuterium isotope shift found in this work for the symmetric C–Br motion in $HCBr_3$ is about 18 cm^{-1}. Thus, the assignment of the bands, HA_3 and DA_3, to the symmetric C–Br stretching mode is reasonable, but this assignment is not as strongly supported as those to ν_5 and ν_6 of dibromomethyl.

A careful search was made for the remaining three vibrations of the radical, but no additional absorptions were found which could be assigned to this species. Sample scattering of the infrared light at higher frequencies prevented the observation of the C–H stretching mode which is expected near 3000 cm^{-1} for $HCBr_2$ and above 2000 cm^{-1} for $DCBr_2$. The other two absorptions of the radical are either too weak to be observed here or lie beyond the low-frequency limit of our spectrophotometer.

Product-Rule Calculations

Product-rule calculations were done for the A'' symmetry block using assignments to ν_5 and ν_6 for the $HCBr_2$ and $DCBr_2$ isotopes, and an average frequency (782.3 cm^{-1}) between the observed matrix splitting for the HA_2 bands for ν_6 of $HCBr_2$. These calculations were performed for angle $HCBr = \text{angle } BrCBr = 109.5°$, 115°, and 120° and the bond lengths from bromoform.[15] The usual cubic contribution to anharmonicity causes the calculated harmonic ratio (D/H) to fall slightly below the observed anharmonic ratio. We find that the observed ratio exceeds the calculated ratio by 0.20% for the three bond angles. This excellent agreement using reasonable structural parameters supports our vibrational assignments to dibromomethyl.

Normal-Coordinate Calculations

Normal-coordinate calculations were performed using the Wilson *FG* matrix method and a least-squares adjustment program FADJ written by J. H. Schachtschneider. Internal coordinates were transformed into the symmetry coordinates listed in the difluoromethyl radical paper.[16] Since both frequencies in the A'' block were observed for $HCBr_2$ and $DCBr_2$, the complete *F* matrix which best fit the observed A'' frequencies was determined for the 115° bond angle estimated earlier in this paper for dibromomethyl. The *F* matrix for the antisymmetric symmetry block for tetrahedral and planar bond angles are also listed in Table VI for comparison. Even though the planar geometry belongs to C_{2v} symmetry, the antisymmetric symmetry coordinates in C_{2v} symmetry are the same as those in C_s symmetry. The excellent agreement between calculated and observed frequencies adds strong support to the antisymmetric vibrational assignments to dibromomethyl.

Unfortunately, we have observed only one frequency in the A' symmetry block, so a rigorous calculation of the symmetric C–Br symmetry coordinate force constant is not possible. However, an approximate value for F_{22} can be calculated by transfering force constants from other similar species for diagonal terms in the *F* matrix and determining the value of F_{22} which best fits the two isotopic assignments to ν_2. In this calcula-

---

[13] G. Herzberg, Proc. Roy. Soc. (London) **A262**, 291 (1961); R. W. Fessenden, J. Phys. Chem. **71**, 74 (1967).

[14] R. W. Fessenden and R. H. Schuler, J. Chem. Phys. **43**, 2704 (1965).

[15] S. Kojima, K. Tsukada, S. Hagiwara, M. Mitushima, and T. Ito, J. Chem. Phys. **20**, 804 (1952).

[16] T. G. Carver and L. Andrews, "Infrared Spectrum of the Difluoromethyl Radical in Solid Argon," J. Chem. Phys. (to be published).

TABLE VI. Force constants for the dibromomethyl radical calculated for several assumed structures.

Structure			Antisymmetric block				Symmetric block						
Angle HCBr BrCBr (deg)	r_{CH} (Å)	r_{CBr} (Å)	F_{55} (mdyn/Å)	F_{56} (mdyn/rad)	F_{66} (mdyn·Å/rad)	$\Delta\nu$[a]	F_{22}[b]	$\Delta\nu$	F_{22}[c]	$\Delta\nu$	Average F_{22}	F_r	F_{rr}
109.5	1.07	1.93	3.25	0.33	0.58	0.6	2.57	28.3	3.48	5.4	3.0±0.5	3.1±0.3	−0.2±0.3
115[d]	1.07	1.93	3.10	0.32	0.50	0.5	3.32	1.0	4.01	2.9	3.7±0.4	3.4±0.3	0.3±0.3
120	1.07	1.93	2.98	0.31	0.44	0.5	3.90	2.5	4.60	0.5	4.3±0.4	3.7±0.3	0.7±0.3

[a] Average difference between calculated and observed frequencies (cm^{-1}).

[b] Millidynes/angstrom, calculated fixing $F_{11}=5.35$ mdyn/Å, $F_{33}=0.503$ and $F_{44}=0.792$ mdyn·Å/rad^2.

[c] Millidynes/angstrom, calculated using approximate separation of high and low frequencies.

[d] Bond angle estimated here for $HCBr_2$.

TABLE VII. Carbon-bromine valence force constants[a] for bromocarbon free radicals and stable molecules.

Molecule	F_r	F_{rr}	F_r-F_{rr}	Reference
CBr_3	3.5±0.3	0.7±0.3	2.85	b
H_2CBr	3.42	···	···	c
$HCBr_2$	3.4±0.3	0.3±0.3	3.10	d
C_2Br_4	3.07	0.31	2.76	e
$HCBr_3$	2.91	0.63	2.28	f
H_3CBr	2.90	···	···	g
H_2CBr_2	2.84	0.19	2.65	h
CBr_4	2.45	0.30	2.15	b

[a] In millidynes per angstrom.

[b] Reference 3 assuming Br–C–Br angle = 109.5°.

[c] Reference 20.

[d] This work assuming angle H–C–Br = angle Br–C–Br = 115°.

[e] G. de Alti, V. Galasso, and G. Costa, Spectrochim. Acta **21**, 649 (1965).

[f] Reference 18.

[g] J. Aldous and I. M. Mills, Spectrochim. Acta **19**, 1567 (1963).

[h] J. M. Dowling and A. G. Meister, J. Chem. Phys. **22**, 1042 (1954).

tion the F_{CH} deduced for the methyl radical[17] was used for F_{11} while F_{33} and F_{44} were taken from bromoform.[18] The approximate separation of high and low frequencies[19] gives another estimate of $F_{22}=4.01$ mdyn/Å. Our experience is that the former method calculates a lower force constant while the latter gives a higher force constant than would be obtained in a rigorous calculation. Thus, we deduce $F_{22}=3.7\pm0.4$ mdyn/Å.

CONCLUSIONS

The potential constants of dibromomethyl are of interest since they contribute to our understanding of the bonding in halomethyl free radicals.

H–C–Br Bending Force Constant

The H–C–Br valence angle bending potential constant for $HCBr_2$ is slightly smaller than the analogous force constant for bromoform[18] and the dichloromethyl radical.[4] The off-diagonal constant between the antisymmetric H–C–Br bend and C–Br stretching modes for $HCBr_2$ is almost identical to that for $HCBr_3$. This interaction force constant is manifested in the large deuterium shift (62 cm^{-1}) for the antisymmetric carbon–bromine stretching mode which is largely due to the interaction of the ν_5 and ν_6 vibrations for $DCBr_2$ rather than solely to a mass effect.

C–Br Stretching Force Constant

Table VII shows that the antisymmetric carbon–bromine stretching force constant (F_r–F_{rr}) for dibromo-

---

[17] L. Andrews and G. C. Pimentel, J. Chem. Phys. **47**, 3637 (1967).

[18] V. Galasso, G. de Alti, and G. Costa, Spectrochim. Acta **21**, 669 (1965).

[19] E. B. Wilson, J. C. Decius, and P. C. Cross, *Molecular Vibrations* (McGraw-Hill Book Co., New York, 1955).

methyl is considerably higher than that for bromoform.[18] The C–Br valence force constant for $HCBr_2$ is determined from F_{55} and F_{22} to be 3.4±0.3 mdyn/Å, somewhat higher than the values between 2.45 and 2.91 mdyn/Å found for the four bromomethanes. F_r for the dibromomethyl radical is near that for the tribromomethyl[3] and bromomethyl[20] radicals. The uncertainty in F_{rr} contributed by the approximate value of F_{22} should be near that given here since F_{rr} ranges between 0.2 and 0.7 mdyn/Å for a number of bromocarbon molecules. Thus, the F_r deduced here for $HCBr_2$ is expected to be accurate within the approximate limits shown in Table VII.

Bonding in Bromomethyl Radicals

As we have pointed out earlier,[3] studies of the bond dissociation energies have suggested that the tribromomethyl radical is electronically stabilized by approximately 12 kcal/mole. Moreover, the C–Br force constant for tribromomethyl exceeds normal C–Br single-bond values. In like manner, bond dissociation energies indicate that dibromomethyl is electronically stabilized,[21] although to a lesser degree than tribromomethyl, which parallels our finding higher than normal C–Br force constants in dibromomethyl. Apparently, trifluoromethyl[21] and difluoromethyl are stabilized very little if any, in line with the observation of normal C–F valence force constants[16] for these fluoromethyl radicals. This contrasts to trichloromethyl and dichloromethyl which are electronically stabilized[21] and have higher than normal C–Cl force constants.[4,5]

We suggested earlier[3,5] that the high C–Br and C–Cl force constants found for CBr_3 and CCl_3 could be attributed to resonance stabilization of these free radicals by participation of the charged structures illustrated by Andrews and Carver[3] for CBr_3. The observation of normal C–F bonds in CF_3 and HCF_2 is consistent with this explanation since the more electronegative fluorine would not be expected to transfer a *single* electron to carbon as readily as would the more polarizable chlorine and bromine atoms. The high carbon–halogen force constants in $HCBr_2$ and $HCCl_2$ can be explained using analogous resonance structures.

However, there is still another difference between fluorine as compared to chlorine and bromine. While fluorine has only *s* and *p* orbitals available for bonding, chlorine and bromine have in addition *d* orbitals in their valence shells. This suggests consideration of additional stabilization of chlorine and bromine bonds to a free-radical carbon involving $(p\text{–}d)$ π bonding between the half-filled orbital on carbon in the radical and the chlorine or bromine *d* orbitals. Such bonding is not possible for fluoromethyl radicals or for normal molecules with completely satisfied valence. The *p* character of the free-radical electron is, of course, dictated by the hybridization of the carbon orbitals and structure of the free radical, which possibly ranges from near sp^3 for CCl_3 and CBr_3 to almost pure *p* for H_2CCl and H_2CBr.

That the *d* orbitals on chlorine and bromine are available for bonding is indicated by the existence of such interhalogen compounds as ClF_3 and BrF_3. However, Jaffe[22] suggests the need for a small positive charge on the *d*-orbital atom to contract its *d* orbitals in order to make them overlap more favorably with *p* orbitals on adjacent atoms. $(d\text{–}p)$ π bonding has been discussed[23] for SiF_4, in which the highly electronegative fluorine atoms produce a polarity in the σ bonds. Consequently, the *d* orbitals of silicon contract, and these orbitals may form π bonds with the extra *p* orbitals on fluorine. However, it has been pointed out that *p–d* orbital overlap is better when the *d* orbital is considerably more diffuse,[23] so the presence of positive charge may not be necessary. $(p\text{–}d)$ π bonding in thiophene between carbon and sulfur need not require any positive charge on sulfur,[23] although the presence of such positive charge has been suggested by the participation of resonance structures.[24]

Even though chlorine and bromine are slightly more electronegative than carbon, any participation of the charged resonance structures of the type illustrated[3] for CBr_3 produces positive charge on the halogen. It should be noted that the electronegativity of "free-radical carbon" is not known and it might easily exceed the electronegativity of carbon with all of its valence satisfied. Thus, if the presence of a small positive charge on bromine and chlorine is necessary to involve their *d* orbitals in $(p\text{–}d)$ π bonding, a mechanism to produce this positive charge is readily available. However, as in the case of carbon–sulfur bonding, this positive charge may not be necessary.[23]

Accordingly, we propose that the enhanced stability of the bromomethyl and chloromethyl free radicals as shown by bond dissociation energies and higher carbon–halogen bond force constants can be attributed to $(p\text{–}d)$ π bonding between the half-filled orbital on carbon and the *d* orbital of appropriate symmetry on bromine and chlorine. The free-radical electron is available for bonding in the $(p\text{–}d)$ π molecular orbital.

---

[20] L. Andrews, work on H_2CBr is in progress.

[21] A. H. Sehon and M. Szwarc, Proc. Roy. Soc. (London) **A209**, 110 (1951).

[22] H. H. Jaffe, J. Phys. Chem. **58**, 185 (1954).

[23] D. P. Craig, A. Maccoll, R. S. Nyholm, L. E. Orgel, and L. E. Sutton, J. Chem. Soc. **1954**, 332.

[24] V. Schomaker and L. Pauling, J. Am. Chem. Soc. **61**, 1769 (1939); H. C. Longuet-Higgins, Trans. Faraday Soc. **45**, 173 (1949).